"A Cochlear Nucleus Auditory prosthesis based on microstimulation"

Contract No. NO1-DC-8-2102
Progress Report # 12 (Final Report)

HUNTINGTON MEDICAL RESEARCH INSTITUTES
NEURAL ENGINEERING LABORATORY
734 Fairmount Avenue
Pasadena, California 91105

D.B. McCreery, Ph.D.
W.F. Agnew, Ph.D.
L.A. Bullara, B.S.
T.G.H. Yuen, Ph.D.

HOUSE EAR INSTITUTE
2100 WEST THIRD STREET
Los Angeles, California 90057
R.V. Shannon
J.K Moore
D. Baskent
L. Friesen
S. Otto

I: Introduction

This is the final progress report and Final Report for contract NO1-DC-8-2102, whose objective has been to complete the pre-clinical development of an auditory prosthesis based on microstimulation within the ventral cochlear nucleus. The work is a collaboration between Huntington Medical research Institutes and the House Ear Institute, with Cochlear Corporation, the U.S. subsidiary of Cochlear Ltd, as a corporate partner.

The version of the auditory brainstem implant (ABI) presently in clinical use can restore useful hearing to patients in whom both auditory nerves have been destroyed by tumors of the VIIIth cranial nerve (vestibular schwannomas), and who therefore cannot benefit from cochlear implants. Type 2 Neurofibromatosis (NF 2) is the most common medical condition that produces bilateral VIIIth nerve tumors. The present version of the ABI consists of 8 platinum-Iridium disk electrodes mounted on a silicone elastomer substrate. Following removal of the vestibular schwannoma, the electrode assembly is placed inside the lateral recess of the IVth ventricle, which positions the electrode adjacent to the cochlear nucleus.

Most ABI patients report different pitch sensations when different electrodes are pulsed, suggesting that these surface electrodes have some limited ability to access the tonotopic dimension of the human cochlear nucleus. However, the overall performance level of patients with the surface-electrode ABI is considerably poorer than the average performance of patients with a multi-channel cochlear implant (CI). The reasons for this large difference in performance between the CI and ABI are not clear, but it may be due at least in part to the limited ability of the surface electrode to access the tonotopic organization of the ventral cochlear nucleus. Penetrating microelectrodes for stimulation of the human cochlear nucleus have been under development for more than 12 years under the preceding NIH contracts in this series. Penetrating microelectrodes will stimulate highly selective areas of the human cochlear nucleus (McCreery et al., 1998). Excellent tonotopic selectivity should be achievable with penetrating electrodes, potentially overcoming a major shortcoming of the surface ABI electrodes.

II: Development of a microstimulating array for the Human cochlear nucleus

II-1: The anatomy of the human cochlear nucleus and the configuration of the penetrating electrode array (Quarterly Progress Reports # 5 & 9).

A major task in achieving the objective of the contract is to specify the configuration of the microelectrode array, including the lengths and spacing of the microelectrodes, as well as the location and direction at which they are to be inserted into the brainstem. Anatomical studies of

the human auditory brainstem were conducted at the House Ear Institute. The neuronal cytoarchitecture of the ventral cochlear nucleus indicates that the electrodes should be inserted into the central area of the nucleus, where the multipolar cells are clustered. Anatomical studies were performed on the cochlear nuclei of persons with normal hearing, and on those from persons with neurofibromatosis 2 (NF2), in whom the auditory nerve had been completely ablated after removal of vestibular schwannomas.

Until recently we had assumed that surgeon must inset the array into the free ventroposterior surface of the VCN. As a landmark for this approach, we first considered the stump of the eighth nerve. As reported in 1998, there were problems with this approach, including postsurgical absence of a nerve stump and angulation of the nerve root. We then modeled electrode insertion using the taenia choroidea as a surface landmark. The taenia choroidea is a membrane formed by fusion of the ependymal inner surface of the lateral recess with the outer pial surface of the brainstem. It is visible to the surgeon and is routinely used to locate the foramen of Luschka in order to place the surface ABI in the lateral recess. Our computer reconstructions of the brainstem confirmed that the taenia consistently overlies the posterior VCN. When the electrodes are inserted along the long axis of the nucleus, the lengths of the shafts should range from 1 to 3 mm, in order to span the tonotopic gradient of the ventral region (QPR # 5).

The possibility of another approach was suggested by neurosurgeon William Hitzelberger. A vestibular schwannoma “dissects” the cerebellum off of the brainstem, leaving the CN in a superficial position, thus opening the possibility of a more lateral approach into the VCN. The complex shape of the nuclei, particularly their flattening in the mediolateral dimension, places significant constraints on the design and placement of an array of penetrating electrodes. The flattened shaped of the human cochlear nuclei over the medial cerebellar peduncle has been advantageous for the use of the surface electrode, since it offers the electrode a greater area of contact. However, a penetrating electrode aimed at the central VCN has a target area with a maximum dimension along any of its axes of only 2-4 mm.

One factor influencing the design of a penetrating electrode is the question of atrophy or distortion of the cochlear nuclei due to loss of the cochlear nerve. Thus it becomes essential to have an accurate description of the size and shape of the cochlear nuclei in deafened individuals. During contracts I and II, we determined shapes and volumes of the cochlear nuclear complex in seven normal persons and eight profoundly deaf subjects. The population of deaf subjects included one with a unilateral schwannoma, but no neurofibromatosis 2 (NF2) subjects. The reconstructions of their cochlear nuclei showed minor variations in the shape of the VCN, but no features were seen that would allow us to distinguish the brains of deaf subjects from those of hearing subjects. During the present contract, we obtained and analyzed the brainstem of an NF2 subject who had undergone bilateral removal of vestibular

tumors 10 and 7 years previously and who has been implanted with a surface ABI device at the time of the second tumor surgery. In this subject, unlike the deaf subjects analyzed previously, there was a significant (30-50%) reduction in the volume of the cochlear nuclei. A related consideration is that the optimal distributions of electrode lengths is somewhat dependant upon the angle at which the arrays is inserted into the nucleus. With a ventral approach, the greatest problem is the extreme narrowness of the nucleus along the mediolateral dimension. If a penetration is not made along the long dimension of the narrow VCN, the tips of longer electrodes are more likely to fall outside the VCN . With a more lateral approach, the electrodes will cross the tonotopic planes of the VCN at about a 45° angle, similar to what would occur with a ventral approach, but they must be short enough so as not to penetrate completely through the narrowed nucleus.

II-2 Effect of overall frequency range and spectral partitioning in subjects with normal hearing (QPR # 9)

Psychophysical studies using subjects with normal hearing and a simulate auditory implant revealed that when an auditory implant is able to convey spectral information, proper matching of spectral bands to electrodes based on pitch percept is essential for good performance on speech recognition tasks. Thus an important consideration in setting up the parameters of a speech processor for the PABI is the assignment of frequencies to electrodes. If the array of electrodes does not produce percepts of pitch that cover the entire frequency range, some accommodation must be made in the frequency assignments.

To better understand the potential importance of these issues we measured vowel and consonant recognition in normal-hearing listeners in conditions designed to simulate possible PABI outcomes. We simulated four different distributions of pitch across penetrating electrodes. For each electrode pitch distribution, we measured speech recognition as a function of the frequency-electrode mapping.

Acoustic simulations were constructed using noise-band speech processors as described by Shannon et al. (1995). The speech signals were digitized at a 22 kHz sample rate and passed through a pre-emphasis filter to whiten the spectrum (6dB/octave decrease below 1200 Hz). The signal was then split into frequency bands (6th order Butterworth filters). The envelope was extracted by half-wave rectification and low-pass filtering (-18 dB/octave filters with a cut-off frequency of 220 Hz). The envelope from each band was then used to modulate wide-band white noise. The modulated noise was frequency-limited by filtering. In some conditions the filters were the same filters used in the analysis bands ("matched" conditions), while in other conditions the band-pass filters were different in center frequency and bandwidth from the analysis filters

Noise carrier bands were designed to simulate the stimulation that might be achieved by

penetrating electrodes. The high spatial localization of stimulation with a penetrating electrode was simulated by a 100-Hz wide carrier band of noise, filtered with 6th order bandpass filters (Butterworth, 36 dB/oct slopes). Four "electrode" outcomes were simulated by four narrow band noise carriers: four electrodes (1) spaced linearly in frequency, (2) spaced logarithmically in frequency, (3) all four clustered at a low frequency, and (4) all four clustered at a high frequency. These four conditions constitute two cases of desirable tonotopic spacing (covering the entire auditory pitch range) and two cases of sub optimal tonotopic spacing (all four electrodes close together in pitch). For each of these electrode spacing conditions we measured consonant and vowel recognition for 6 different partitions of the frequency range from 100-7000 Hz, ranging from linear frequency spacing of the four bands to logarithmic spacing . An additional condition measured speech recognition for the high- and low-frequency clusters when the analysis filters were matched to the carrier bands.

Phoneme recognition performance was assessed using two sets of speech materials: medial vowels and medial consonants. Vowel recognition was measured in a 12-alternative identification paradigm, including 10 monophthongs and 2 diphthongs, presented in a /h/-vowel-/d/ context, e.g., "heed", "hid", "hayed", "head", "had", "hod", "hawed", "hoed", "hood", "who'd", "hud", "heard".

The results for consonant and vowel recognition show the importance of matching the analysis frequency partition to the tonotopic location of the electrodes. Both consonant and vowel recognition were poor for the high-pitch cluster. Consonant recognition was poor, but vowel recognition was reasonable for the low-pitch cluster when the tonotopic bands were matched to the carrier bands, i.e. the simulated condition in which the analysis bands are matched to the electrode pitch. The high-frequency and low-frequency clusters produce poor performance for all frequency divisions. This result has important implications for the design of penetrating electrode system, i.e., it is important to achieve a wide range of pitch across the penetrating electrodes.

Overall, there was a strong effect of both analysis and carrier band spacing for vowel and consonant recognition. Best performance was obtained when the carrier bands (simulated electrodes) spanned the entire frequency range logarithmically and when the analysis bands were also divided approximately logarithmically. From previous work we know that at least one band division near 1500 Hz is critical for good vowel recognition. These results imply that penetrating electrode systems should be designed so that the electrodes have the best chance of spanning the entire frequency range and are equally spaced in logarithmic frequency. The normal auditory tonotopic map in the cochlea is organized approximately according to log frequency and the "Greenwood mapping" is propagated through all auditory brainstem nuclei. While we cannot know the exact tonotopic map of the human cochlear nucleus, we assume that the "Greenwood tonotopic map" is preserved, but scaled to the size

of the nucleus. The primary tonotopic axis of the human posterior-ventral cochlear nucleus (PVCN) is orthogonal to the surface of the brainstem and is approximately 2-3 mm in extent (see Section 1 of this QPR). Ideally, penetrating microelectrodes should be designed so as to span the entire tonotopic range, in equal increments. Our analysis of normal human brainstems and brainstems following single and bilateral vestibular schwannomas suggest that penetrating electrodes should range in length from 1.0 mm to 3.0 mm in order to span the entire range of acoustic frequencies when the electrodes is inserted along a dorso-ventral direction. They should be slightly shorter in order to span the axis if the array is inserted more laterally. Our present design contains two 3 mm stabilizing pins and 8 active electrodes, staggered in length between 1 and 2 mm. Depending upon the angle of insertion, this array may not span the entire tonotopic axis of the VCN. However, this error will cause a loss of access to the portions of the VCN representing high acoustic frequencies; a condition that is preferable to losing access to the lower frequencies, as would occur if the electrodes were to pentrate too deeple into the nucleus.

II-3: Histologic evaluation of electrode arrays sized for the human cochlear nucleus (QPR s #1, 6,8 &10).

We have developed a hand-held insert tool which will allow the surgeon to implant the arrays into the human cochlear nucleus, through the narrow opening provided by the translabyrinthine approach to the brainstem (QPR #1).

The feline ventral cochlear nucleus contains cell types that are very similar to those in the human VCN, but it is not a good site in which to evaluate the human array and the inserter tool, due to its shape and location as a pendulous structure on the dorsolateral surface of the brainstem. We have therefore implanted the human-type cochlear nucleus arrays into the feline lumbar spinal cord and also into the cerebral cortex. For this type of evaluation, the spinal cord is probably the best feline model for the human auditory brainstem, but one difference is that it is covered by dura rather than by the lateral cerebellum, as is the human auditory brainstem (cats have only a small subarachnoid space over their lumbar enlargement). The second site, the feline cerebral cortex, allows us to evaluate the arrays when they are implanted into very vascular brain tissue. Also, the cortical gray matter spans nearly the same range of depths beneath the pia as does the human ventral CN. We used the hand held inserter tool to implant arrays of microelectrodes into the feline cerebral cortex and spinal cord. The lengths of the electrodes (1 to 3 mm) was selected to span most of the tonotopic gradient of the human cochlear nucleus.

The microelectrodes used in these studies had rather blunt tips (radius of curvature of 5-6 μm) in order to minimize damage to the small blood vessels. Six arrays of iridium microelectrodes were implanted for 30 to 35 days into cat lumbar spinal cord. Histologic

analysis revealed some injury in both gray and white matter within 25 to 50 μm the electrode shafts and dorsal to the tips of the shorter microelectrodes, but the neurons and neuropil immediately ventral to the tip sites (the electrodes' active stimulating sites) appeared to be normal. Longer electrodes induced more injury, especially when they penetrated into white matter. Based on these findings, we have reduced the lengths of the array's "stabilizing pins", to 3 mm. As noted in the previous section, we also have decided to reduce the range of the lengths of the working electrodes, to 1 to 2 mm.

We have examined 40 electrode tracks from 6 such arrays implanted for 30 to 67 days in the cerebral cortex , and we have found little evidence of new or resolved hemorrhages (erythrocytes or hemosiderin). Neurons within 25 to 50 μm of the tips sites appear quite normal. In cat CNH7, a few very small aggregates of hemosiderin were observed near 3 or 4 of the cortical capillaries, 30 days after implanting the arrays, but no evidence of space-occupying microhemorrhages. No hemosiderin or erythrocytes was observed in any of the histologic sections from cat CNH12 or CNH15. Only one of the 40 tracks was accompanied by a small glia scar whose shape of suggests that it may have originated from a healed microhemorrhage, and in this case the scar is small and is surround by normal-appearing tissue. These findings indicate that the amount of tissue injury that will be inflicted by an array of microelectrodes inserted into the human CN, using the hand-held tool, will not seriously compromise the functionality of the auditory prosthesis. In particular, there will be healthy neurons and axons within 25 μm (at most 50 μm) of the electrode tips. These findings speaks well for the safety of implanting the arrays using the hand held tool.

III: Animal studies of stimulus parameters for safe and effective intranuclear microstimulation

III-1: Physiologic and histologic effects of prolonged microstimulation in the feline ventral cochlear nucleus (QPR # 2,4,7,10 and McCreery et al, 2000)

These studies were conducted to define the range of stimulus parameters that can be used safely with an array of intranuclear microelectrodes. We chronically implanted activated iridium microelectrodes with geometric surface areas of approximately 1,000 μm^2 into the feline posteroventral cochlear nucleus (PVCN) and a recording electrode was implanted into the contralateral inferior colliculus. Beginning 80 to 250 days after implantation, the microelectrodes in the PVCN were pulsed for 7 hours per day, on up to 21 successive days. For these stimulation regimens, we simulated an acoustic environment based on a computer-generated artificial voice that reproduces many of the characteristics of real speech. The artificial voice signal is logarithmically compressed and then sets the amplitude of the charge-

balanced stimulus pulses. The artificial voice signal was presented for 15 seconds, followed by 15 seconds in which the stimulus amplitude was held near the threshold of the evoked response (14 μA with a stimulus pulse duration of 40 μs/phase, 6 μA with a pulse duration of 150 μs). The 50% duty cycle is intended to simulate a moderately noisy acoustic environment. The pulse rate (250 Hz per electrode) and the maximum pulse amplitude were selected as those that are likely to provide a patient with useful auditory percepts.

"Non-embedded" evoked responses evoked from the microelectrodes in the PVCN were recorded in the inferior colliculus, before and also immediately after the daily 7-hour sessions of stimulation. They were generated using a 50 Hz "probe" stimulus (a much lower frequency than the 250 Hz used during the 7-hour stimulation session). They are designated "non-embedded response growth functions" since they were not acquired during the 7-hour session, and thus not contemporaneously with the artificial voice signal,

"Embedded" evoked response also were acquired during the first hour of the regimen, and during the last hour of each of the 7- hour sessions, while stimulating with the artificial voice signal (the "test stimulus"), and at the full rate of 250 per electrode. The procedure by which they are acquired is described in McCreery et al, (2000) and in previous quarterly reports.

Response growth functions (RGFs) were generated by plotting the amplitude of the various components of the averaged evoked responses (AERs) against the amplitude of the evoking stimulus. The amplitude of an evoked response was measured from the negativity to the peak of the subsequent positivity, as illustrated in Figure V-1-1A.

The changes in the non-embedded RGFs reveal depression of neuronal excitability (SIDNE) that persists after the end of the 7 hours of high-rate stimulation with the artificial voice signal, and may help to identify stimulation protocols that place inordinate stress on the neurons of the ventral cochlear nucleus. The changes in the embedded RGFs reveal how the regimen of prolonged stimulation affects the neurons' responses to the actual artificial voice signal . The non-embedded and embedded responses, and the histologic evaluation of the implant sites, together provide a picture of the safety and efficacy of the stimulation regimen.

The stimulation and data acquisition was conducted using a two-way radiotelemetry stimulation and data acquisition system, and the cats are able to move about freely in a large Lucite cage.

The changes in neuronal responses during the multi-day stimulation regimens were partitioned into long-lasting, stimulation-induced depression of neuronal excitability (SIDNE), and short-acting neuronal refractivity (SANR). Both SIDNE and SANR were quantified from the changes in the RGFs recorded in the inferior colliculus.

All of the stimulation regimens that we evaluated induced measurable SIDNE and SANR. The combined effect of SIDNE and the superimposed SANR is to depress the neuronal response near threshold, and thereby, to depress the population response over the entire

amplitude range of the stimulus pulses. SIDNE and SANR may cause the greatest degradation of the performance of a clinical device at the low end of the amplitude range, and this may represent an inherent limitation of this type of spatially localized, high-rate neuronal stimulation.

iSIDNE was quantified as the % change relative to the pre-stimulus response growth function. iSANR was quantified as the % change relative to the non-embedded growth function acquired at the end of the daily session. iTOTAL, the index for the combined effect of the SIDNE and SANR, was the % change relative to the prestimulus non-embedded growth function. The indices of SIDNE and SANR ("iSIDNE, iSANR"), and the effective sum of the two (iTOTAL"), are summarized in Table III-1-1, for the four stimulation protocols that we evaluated. Values are means, ± the standard deviation. The number of electrodes in the group is indicated in parentheses.

TABLE III-1-1

Protocol	Stimulus amplitude (range)	Pulse duration	iSIDNE, First day	iSIDNE, Last day	iSANR, First day	iSANR, Last day	iTOTAL, First day	iTOTAL, Last day
A	6-20 µA	150 µs	8.1%±10%(12)	5.3%±11%(12)	19%±7.5% (4)	19%±8.1% (4)	22%±5.6% (4)	23%±10% (4)
B	6-32 µA	150 µs	65%±24% (4)	73%±26% (4)	32%±18% (4)	43%±21 % (4)	76%±16% (4)	80%±13% (4)
C	14-48 µA	40 µs	2.4%±1.7% (6)	0.6%±2.1% (6)	16%±9.7% (4)	12%±12% (4)	25%±3.3% (4)	25%±8.4 (4)
D	14-63 µA	40 µs	19%±13% (8)	20%±13% (8)	21%±8.1% (4)	18%±6.1% (4)	30%±4.4% (4)	33%±4.8% (4)

Protocols A & B employed a long (150 µs) stimulus pulse duration and relatively low pulse currents. Protocols C & D employed a short pulse duration (40 µs) and higher pulse currents. Protocol B used a greater range of pulse amplitudes than protocol A, and protocol D used a greater range than C. The indices of SIDNE are significantly different for protocols A & B, and also for C & D. ($p<0.001$ for the contrast between A&B, $p<0.01$ for the contrast between C & D). For none of the protocols was the SIDNE significantly different between the end of the first day and last day of the regimen ($p>0.5$). Between protocols A & B, the combined effect of the SIDNE and SANR (iTOTAL) also was significantly different, both on the first and last days ($p<0.01$). Between protocols C & D, iTOTAL was not significantly different ($p=0.19$ on first day, $p=0.14$ on last day) but this may have been due to the low power of the t-test, due to the small number of electrodes in each group. Protocols A and C preserved most of the dynamic range of the neuronal response when using either long (150µs/phase) or short (40 µs/phase) stimulus pulses, respectively. Thus, increasing the amplitude of the stimulus (Protocols B and D) was relatively ineffective as a means of increasing the dynamic range of neuronal response, since the greater stimulus amplitude induced more SIDNE . However, protocol D did afford the

greatest dynamic range.

All of the pulsed and unpulsed electrode sites were examined histologically, and no neuronal changes attributable to the stimulation were detected. There was some aggregation of glial cells immediately adjacent to some of the electrodes that were pulsed with the short-duration pulses, and at the highest current densities. However, we have not observed this gliotic reaction in more recent experiments in which the electrode surface area was increased 2,000 μm^2, and we have selected this value for the surface area for the first generation human array.

III-2: Prolonged pulsing of microelectrodes after long-term residence in a cat's cochlear nucleus (QPR # 10)

We next conducted a stimulation regimen spanning 28 days, in a cat in which the microelectrode arrays had been implanted in the posteroventral cochlear nucleus for 374 days. We had 3 objectives in this study:

1.Verify that the evoked neuronal responses are stable during an extended stimulation regimen using intranuclear microelectrodes that had been implanted for more than one year.

2.Determine the extent to which the dynamic range of the neuronal response can be expanded by increasing the range of the stimulus pulse amplitude.

3.Determine if there is less stimulation-induced depression of neuronal excitability near the threshold of the neuronal response when acoustic silence is mapped to a stimulus pulse amplitude of 0 rather than to a value that is close to the threshold of the neuronal responses, as we have done in previous experiments. Another objective was to further elucidate the mechanisms that are responsible for stimulation-induced depression of neuronal excitability.

Two of the microelectrodes in the PVCN were pulsed for 7 hours per day on 29 successive days. The stimulus was charge-balanced cathodic-first pulse pairs, of 40 μs per phase, and the pulse amplitude was modulated by a simulated human voice. The artificial voice signal was presented for 15 seconds, followed by 15 seconds in which the stimulus amplitude was held near the threshold of the evoked response (14 μA with a stimulus pulse duration of 40 μs/phase or else at 0 μA). The pulsing rate was 250 Hz per electrode, and the electrodes were pulsed sequentially (interleaved). The cat received the regimen of stimulation outlined below:

Days	*Range of pulse amplitudes (*)*	*Silence mapped to: (~)*
1-9	14-48 μA	0 μA
10-16	14-63 μA	0 μA
17-23	14-63 μA	14 μA
24-28	14-63 μA	0 μA

(*) As generated by the logarithmically-compressed artificial voice signal

(~) Also specifies level during 15 of every 30 seconds, according to the 50% duty cycle of the artificial voice signal.

The results showed that, as in the earlier study, the dynamic range of the neuronal response evoked by the intranuclear microstimulation was slightly greater when the stimulus amplitude ranged up to 63 μA (vs 48 μA), in spite of slightly more depression of neuronal excitability. Also, the total dynamic range of the neuronal response was slightly greater when (near) silence was represented by a stimulus pulse amplitude of 0 μA rather than by a pulse amplitude that is close to the threshold of neuronal responses (e.g., 14 μA). However, it appears that only a slight advantage is to be gained by the discontinuous mapping procedure, and only those microelectrodes for which the threshold of the neuronal response initially was lower than the low end of the stimulus range would be affected. Even for this circumstance, only the extreme low end of the response range was affected.

We had shown previously that persisting stimulation-induced depression of neuronal excitability, as revealed by a persisting shift in the non-embedded response growth function, is linked closely to the stimulation-induced activation of the neurons of the ventral cochlear nucleus. The present results indicate that this also is true for the dynamic component of the depression, as revealed by a shift in the embedded RFG.

III-3: Evaluation of long-term implant in the feline cochlear nucleus (QPR #8)

We sacrificed cat cn74, seven years and one month after implanting 3 iridium stimulating microelectrodes into the posteroventral cochlear nucleus. The threshold of the electrical response evoked from one of the microelectrodes had remained very stable throughout the first 5 years of implantation, whereupon the electrical connection between the electrode and the percutaneous connector was lost. Another stimulating microelectrode continued to function well, and its response growth function remained very constant throughout 7 years. During the final few months *in vivo*, the threshold of the evoked response increased slightly, to approximately 8-10 μA. This longevity of the intranuclear electrodes is encouraging. Histologic evaluation revealed that the electrode shafts and tips were surrounded by gliotic sheaths that were not more than 10 μm in thickness, and this is consistent with the low threshold of the electrically-evoked response. Neurons and neuropil outside of the sheath appeared to be healthy, and this is consistent with the stable slope of the response growth functions through the 7 years *in vivo*.

IV: Speech Processor Design and Fitting Issues (QPRs # 3 & 11)

IV-1 Number of electrodes and channels

The overall performance level of patients with the existing surface-electrode ABI devices is relatively poor compared to patients with cochlear implants. Although the surface-electrodes ABIs use an arrays 8 to 21 electrodes and most individual patients have more than 4 usable electrodes, few ABI patients are demonstrating performance levels expected from more than 2-3 spectral channels. To assess ABI patients' ability to use spectral information conveyed by multiple electrodes we measured speech recognition performance in one ABI patient with 2, 4, and 9 electrodes. The results, presented in Figure IV-1-1, show an improvement in performance as the number of electrodes was increased from 2 to 4, but no further improvement as the number of electrodes was increased from 4 to 9. When speech spectral bands was assigned to electrodes at random, the patient's performance was even poorer than when only 2 electrodes were used, and assignment of spectral bands to electrodes was ordered according to pitch rank order. This suggests that ABI patients are making some use of tonotopic information, although still in a limited way when compared to patients with cochlear implants. This result also suggests that the frequency-to-electrode assignment is an important factor in ABI performance. The following study was undertaken to assess several methods for assigning frequency regions to ABI electrodes.

IV-2: Matching spectral frequency to electrode pitch

A primary motivating factor for developing penetrating ABI electrodes is to achieve better access to the tonotopic organization of the ventral cochlear nucleus. However, it is possible that one factor that contributes to the poor speech recognition performance in ABI patients is that the pitch sensations of the electrodes are unevenly spaced. In a cochlear implant the electrode is positioned inside the cochlea and along the normal tonotopic gradient that exists along the cochlea. In the surface ABI system there is no clear link between electrode location and pitch, because the normal tonotopic axis of the human cochlear nucleus is orthogonal to the main axis of the electrode array. In some ABI patients pitch increases in the medial-to lateral direction along the electrode array, while in others it is the reverse. In some patients there are a few electrodes that are quite distinct in pitch and others that are quite similar in pitch and quality.

We performed a series of experiments to determine if ABI performance was limited by a poor match between the frequency region of speech and the pitch of each electrode. We asked several ABI patients to estimate the pitch of each electrode on a scale of 0 to 100. We estimated the pitch separation and spacing of the ABI electrodes from the average reported pitch. We then divided the speech frequency spectrum into bands that reflected the relative

difference in pitch of the electrodes. We tried several different mappings – one that tried to match the absolute pitch range and distribution of the electrodes in an individual patient, and one that used the entire frequency range of speech, but divided the frequency-to-electrode assignments in a way that preserved the relative pitch distances between electrode. These results were presented in QPR#3, and showed no improvement in performance for any of the pitch-matching strategies.

IV-3 Effect of stimulation rate

In cochlear implants the effect of stimulation rate on performance is not completely clear, but there are theoretical reasons to expect that high stimulation rates could be beneficial. In the penetrating electrode ABI there is an additional concern that high stimulation rates may cause SIDNE. To investigate the potential beneficial or detrimental effects of stimulation rate we measured speech recognition as a function of stimulation rate in two patients with the present surface electrode ABI. These patients had the Nucleus-24 multichannel ABI device, which allows manipulation of stimulation rate. We measured consonant, vowel and word recognition as a function of stimulation rate for 4-, and 8-electrode speech processors in two ABI patients. Performance was assessed at 250 pulses/sec/electrode (PPSE), at the highest possible rate and at one intermediate rate. Results from one patient were reported in QPR#11. These results showed no significant change in performance as a function of stimulation rate. Figure IV-3-1 presents the results from a second ABI patient, who exhibited relatively good performance with their ABI. The dashed line in each panel indicates the level of performance with the clinical processor that this patient had worn for more than 6 months. Consistent with the results from the initial patient, this patient showed no systematic change in speech recognition performance with stimulation rate. Overall, this patient performed significantly better than the first patient, yet neither showed any effect of stimulation rate.

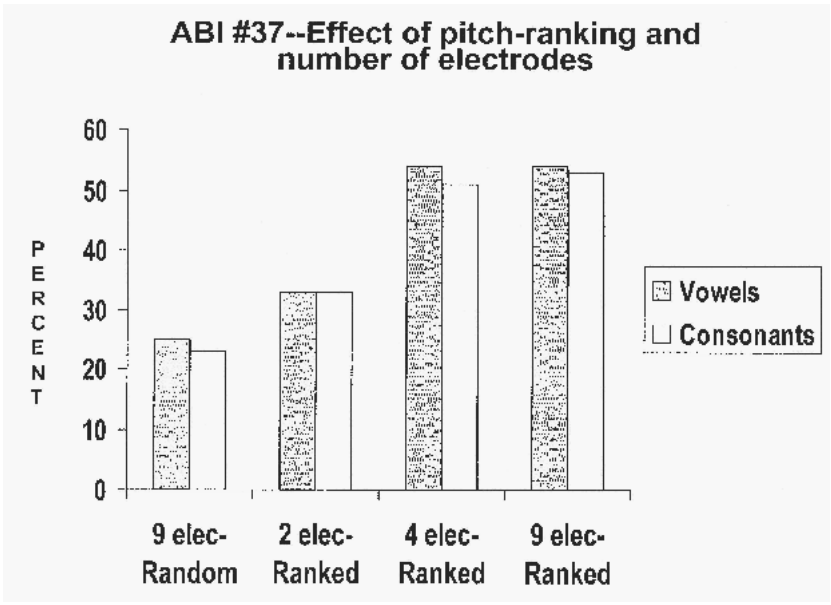
ABI #37--Effect of pitch-ranking and number of electrodes
PERCENT
60
50
40
30
20
10
0
Vowels
Consonants
9 elec- Random
2 elec- Ranked
4 elec- Ranked
9 elec- Ranked

Figure IV-1-1

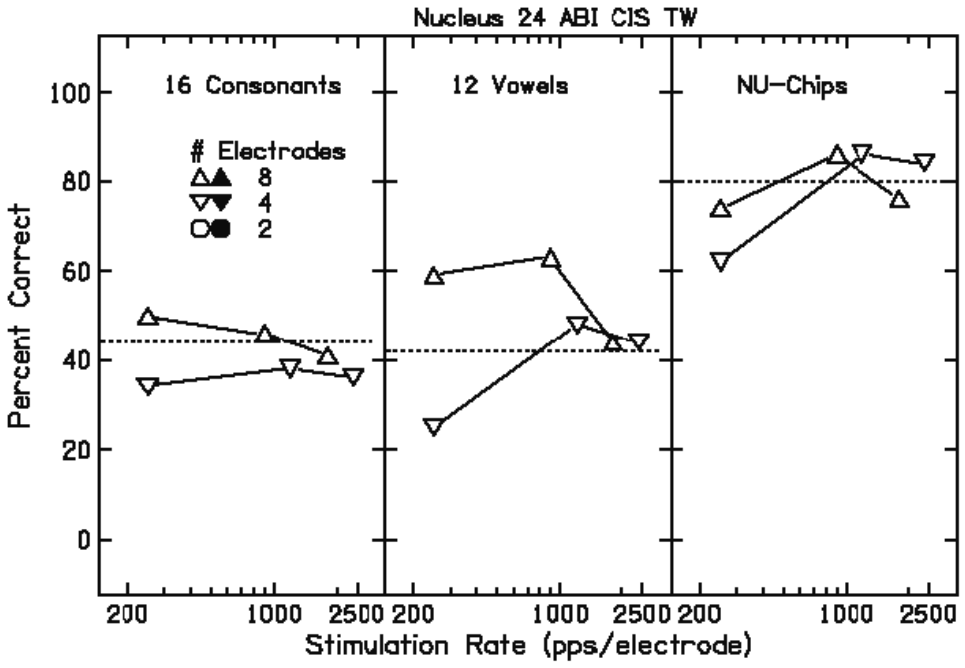
Nucleus 24 ABI CIS TW
16 Consonants
12 Vowels
NU-Chips
Electrodes
8
4
2
Percent Correct
100
80
60
40
20
0
200
1000
2500
Stimulation Rate (pps/electrode)

V: Results not previously reported

V-1: Physiologic effects of high-rate stimulation in the Feline cochlear nucleus.

As noted above and in QPR #11, some data from patients in Poland in whom electrodes had been implanted onto the surface of the cochlea nucleus demonstrated exceptional open-set speech recognition, and one possible explanation is the very high rate of stimulation (1,000 Hz). In animal studies, we have found that a pulse rate in excess of 250 Hz per electrodes induces marked depression of neuronal excitability (SIDNE). However, we had not evaluated pulsing rates as high as 1,000 Hz, and it is possible that this high would cause the neurons of the ventral CN to respond in a stochastic manner (fewer that 1 action potential/stimulus pulse) and the therefore the SIDNE might be less that would be expected on the basis of extrapolation from the our experience with lower pulsing rates.

METHODS

Iridium stimulating microelectrodes with blunt tips (radius of curvature of 5 to 6 µm) were fabricated from lengths of pure iridium wire 70 µm in diameter. The entire shaft and wire junction is coated with 3 thin layers of Epoxylite 6001-50 heat-cured electrode varnish. The insulation was removed from the tip with a laser, leaving an exposed geometric surface area of 2000 +/- 400 μm^2. The individual electrodes were assembled into an integrated array of 4 microelectrodes spaced approximately 400 µm apart. Using general anesthesia and aseptic technique, a pair of stainless steel recording electrodes was implanted by stereotaxic into the right inferior colliculus. The array of 4 iridium stimulating microelectrodes was implanted into the left posteroventral cochlear nucleus (PVCN).

Data were obtained from 2 cats (cn139 and CN141) at 20 and 18 months after implanting the electrodes. In each cat, one of the microelectrodes was pulsed for 7 hours per day, first at 250 Hz, and increasing to 1,000 Hz. The stimulus was charge-balanced cathodic-first pulse pairs, of 40 µs per phase, whose amplitude was modulated by a simulated human voice, as described above. The artificial voice signal was presented for 15 seconds, followed by 15 seconds in which the stimulus amplitude was held near the threshold of the evoked response.

“Non-embedded” evoked responses were recorded in the inferior colliculus in response to the microstimulation in the PVCN, before and also immediately after the daily 7-hour sessions of stimulation. They were generated using a 50 Hz “probe” stimulus (a much lower frequency than the 250 Hz or 1,000 Hz used during the 7-hour stimulation sessions).

“Embedded” evoked response also were acquired during the first hour of the regimen, and during the last hour of each of the 7- hour sessions, while stimulating with the artificial voice signal (the “test stimulus”), and at the full rate of 250 or 1,000 Hz per electrode. The procedure

by which they are acquired is described in McCreery et al, (2000) and in previous quarterly reports.

Response growth functions (RGFs) were generated by plotting the amplitude of the various components of the averaged evoked responses (AERs) against the amplitude of the evoking stimulus. The amplitude of an evoked response was measured from the negativity to the peak of the subsequent positivity, as illustrated in Figure V-1-1A.

The stimulation and data acquisition was conducted using a two-way radiotelemetry stimulation and data acquisition system, and the cats are able to move about freely in a large Lucite cage.

RESULTS

The first study was conducted in cat CN140, 18.5 months after implanting the electrodes. In this animal, the electrode array was in the rostral part of the PVCN. Figure V-1-1A shows a family of "non-embedded" averaged evoked responses recorded in the right inferior colliculus while stimulating with microelectrode #1 in the left posteroventral cochlear nucleus (PVCN). The duration of each phase of the biphasic current pulse was 40 μs. The numbers near the right edge of each trace indicates the amplitude of the evoking stimulus pulse. The responses were acquired before the first 7-hour session of stimulation with the artificial voice signal. Each trace was obtained by averaging 1,024 successive responses. At least 4 response components can be identified in the traces, the first three of which are labeled. Because of its short latency (<1 ms), the first component certainly represents neuronal activity evoked directly by the intranuclear microstimulation in neurons projecting directly to the inferior colliculus (without an intervening synapse). This probably also is true for the second component which has a latency of slightly greater than 1 ms. The third component probably represents neuronal activity that is evoked transsynaptically.

Electrode #1 was pulsed for 7 hrs/day on each of 4 successive days, and the pulse amplitude was modulated between 9 and 48 μA by the logarithmically-compressed artificial voice signal. Note that the lower end of this range was slightly below the threshold of the first component of the evoked response. Figure V-1-1B shows the non-embedded RFG of the first component of the AER, recorded before any stimulation ("baseline RGF") and also the "embedded" RGF recorded during the last hour of the fourth day of the regimen, and the non-embedded recorded immediately after the 4th day. Figures V-1-1C and V-1-1D show the corresponding data for the 2nd and 3rd components. The separation between the baseline RGF and the non-embedded RGF recorded after the 4th day is an index of persisting depression of neuronal excitability, the phenomenon that we have dubbed "SIDNE." For the first two components, SIDNE is minimal. As is typically the case, the effect of the stimulation was most noticeable in the late (3rd) component, which presumably represents neuronal activity this is

evoked transynaptically. The separation between the embedded RGF and the non-imbedded RGF acquired after the end of that 7-hour session is an index of short-acting neuronal refractivity (SANR). As expected, the third component to the response exhibited the most SANR

On days 5 through 16, the pulsing rate with the artificial voice signal was increased to 1,000 Hz. The stimulus amplitude was increased in 3 steps, over an interval of 5 days, up to the original full range of 9-48 μA. The stimulus amplitude was increased in steps because the cat appears initially to have been startled by the high-rate stimulation. Figures V-1-E,F, show the baseline RGF, and the embedded and non-embedded RGFs recorded near the end of, and after, the 13th day of stimulation (the 4th day for which the stimulus range was the full 9-48 μA), for the first and 3rd components of the AER. The threshold of the first component of the non-embedded and embedded components had become elevated, to greater than 30 μA, indicating considerable SIDNE. The threshold of all of the components of the embedded response also was elevated to greater than 30 μA. Thus, during the 1,000 Hz stimulation with the artificial voice signal, the neurons of the PVCN appeared not to be responding over most of the range of the input signal.

During the 14th, 15th and 16th days, we shifted the range of the artificial voice signal so as to modulate the stimulus between 20-48 μA. This was done in an attempt to better utilize the remaining portion of the response range. However, by the end of the 16th day, the embedded responses had become further depressed (Figures V-1-1G,H)

The second part of the study was conducted using cat CN139, 20 months after implanting the microelectrode array. Figure V-1-2A shows the non-embedded averaged evoked responses recorded before the first day of stimulation with the artificial voice signal. In this cat, the stimulating microelectrodes were slightly more caudal in the PVCN than in cat CN140 described above, and the evoked potentials in the inferior colliculus were slightly different. In particular, only the first component is of sufficiently short latency for us to be confident that it was evoked directly rather than transsynaptically. The threshold of all of the components were rather high (approximately 26 μA). Stimulating at 250 Hz for 7 hours was then initiated, with the artificial voice signal modulating the stimulus amplitude between 20 and 63 μA. By the end of the second day of this regimen, the non-embedded and embedded RGFs of the 1st and 2nd component were only slightly separated, indicating only minimal SIDNE and SANR (Figures V-1-2B,C). As is always the case, the late (3$^{rd)}$ component exhibited more SIDNE and SANR (Figure V-1-2D). However, the neurons in the PVCN remained responsive over essentially the full dynamic range of the artificial voice signal.

On the third day, the pulse rate was increased to 1,000 Hz and the stimulus amplitude was titrated up to the original range of 20-63 μA in two steps spanning 2 days. By the end of the second day, the threshold of all components of the embedded response were

considerably elevated and their amplitudes were greatly reduced (Figures V-1-2E,F,G). The neurons of the PVCN had become nearly unresponsive over most of the dynamic range of the stimulus, showing that the high-rate stimulation had induced considerable SIDNE.

In summary, while the neural responses evoked from the medial and caudal parts of the PVCN in these two cats did differ somewhat, in both animals the high-rate stimulation engendered a marked loss of neuronal responsiveness over most of the range of stimulus amplitude, as indicated by a marked increase in the absolute threshold of the neuronal responses. While the decrease in the amplitude of the components might be attributed at least in part to increased temporal dispersion of the action components that comprised these responses, the increase in the absolute thresholds of even the short-latency, directly-evoked responses is disconcerting. These results suggest that stimulation at a very high rate (e.g., 1000 Hz) would not be appropriate for an auditory prosthesis that is based on intranuclear microstimulation. This conclusion is bolstered by the psychophysical studies in which patients with surface ABI electrode arrays did not exhibit improved performance with high-rate stimulation (QPR #11 and Section IV-2).

cat cn140
Non-embedded response before any stimulation

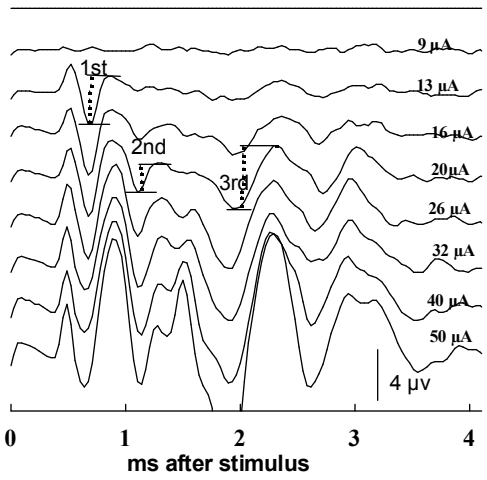

Figure V-1-1A

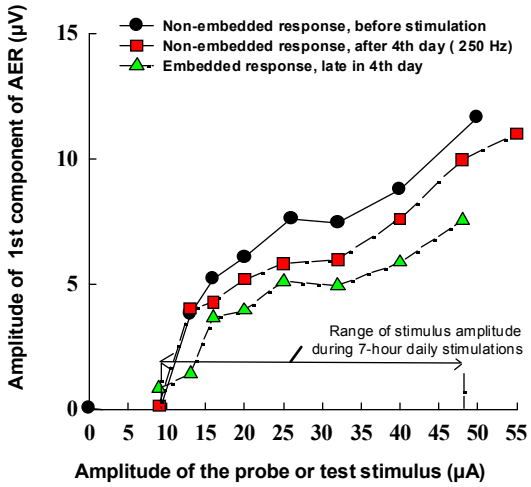

Figure V-1-1B

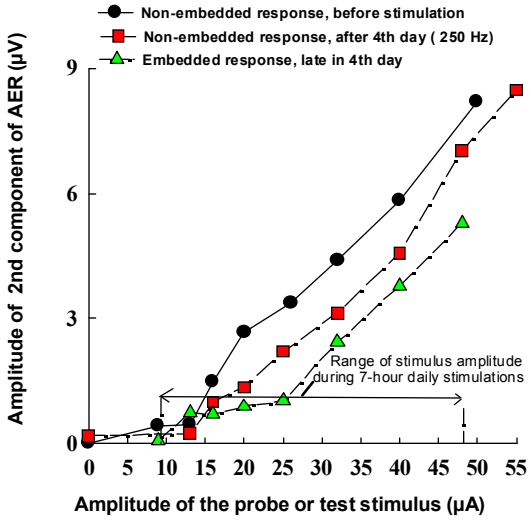

Figure V-1-1C

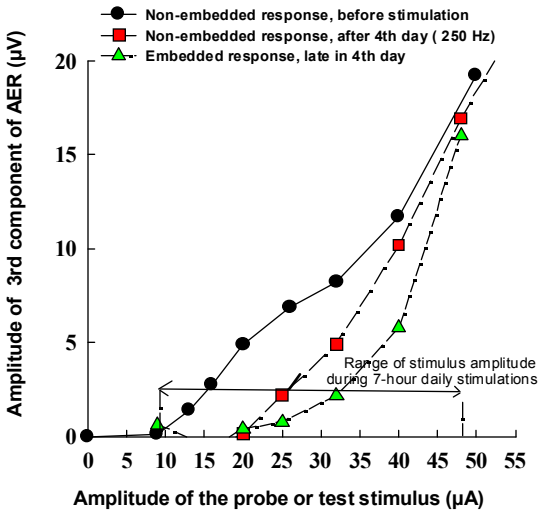

Figure V-1-1D

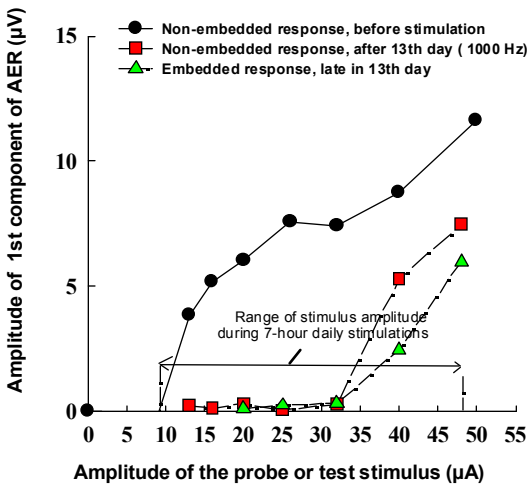

Figure V-1-1E

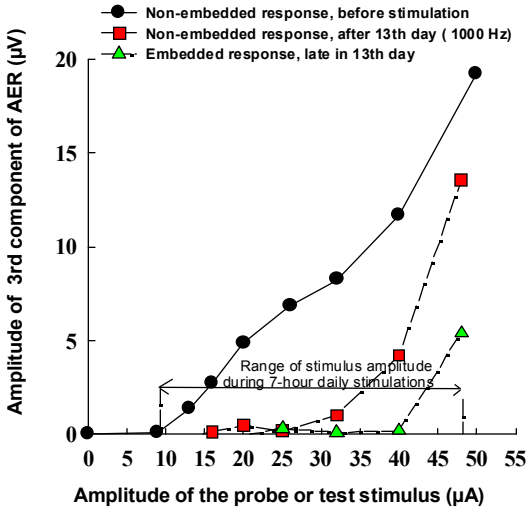

Figure V-1-1F

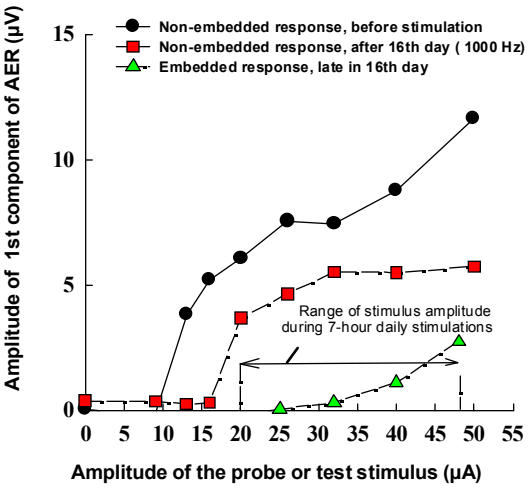

Figure V-1-1G

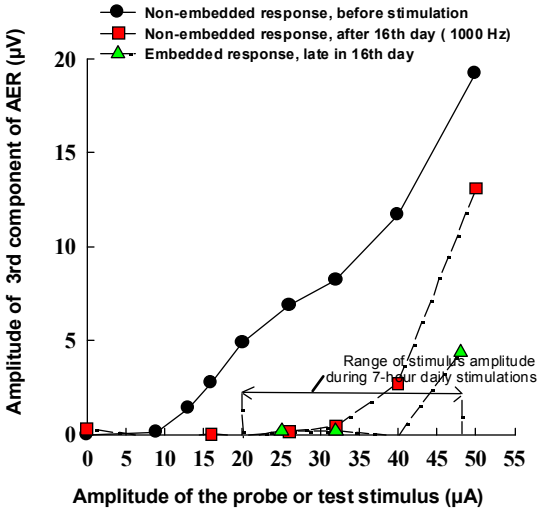

Figure V-1-1H

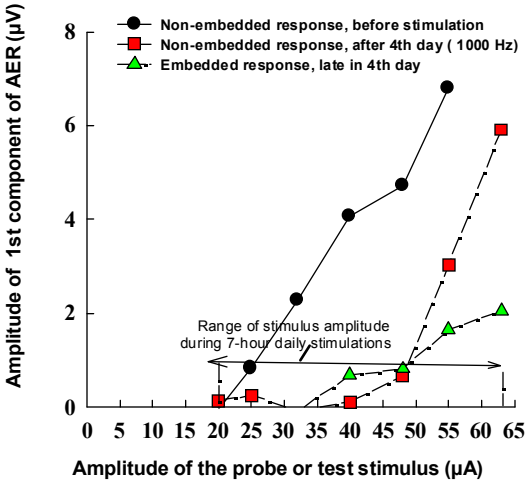

Figure V-1-2E

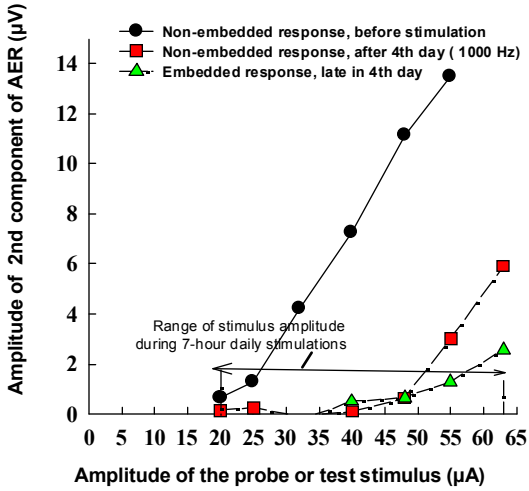

Figure V-1-2F

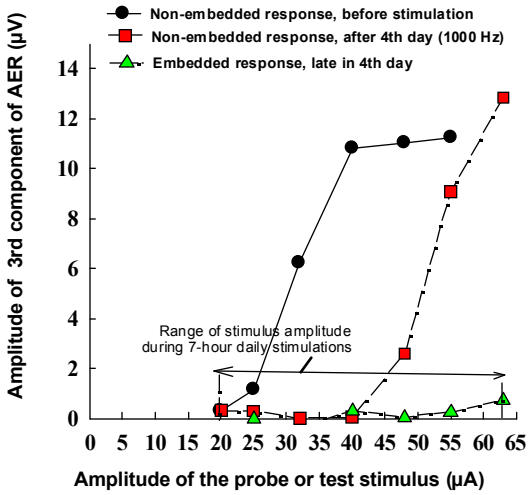

Figure VI-1-2H

V-2: Evaluation of materials for the human microstimulating array

The human penetrating ABI electrode array will be implanted along with an array of surface electrode. The implantable stimulator and the electrode arrays will be manufactured by Cochlear Ltd, using microelectrodes fabricated at HMRI, and suing the physical dimensions determined from studies conducted at HEI and HMRI .

We have developed procedures for fabricating the microelectrode array using materials which carry USP Category VI classifications. Previously, we have insulated our microelectrodes with Epoxylite 6001 varnish, which does not carry this classification. We have adapted a procedure for coating the electrodes with Parylene C, after enhancing the adhesion of the Parylene to the metal by plasma-cleaning the metal surfaces and then priming the surfaces with a methoxysilane (Silquest-A174). This enhanced adhesion is necessary because the personnel at Cochlear Ltd determined that the adhesion of Parylene deposited without enhancement is incompatible with certain operations that are an integral part of their manufacturing procedure. They have found that the physical performance of the adhesion-enhanced Parylene to be adequate, and we have begun animal tests to verify the biocompatibility of this material in brain.

V-3: Evaluation of the positional stability of the array-cable assembly

The positional stability of the implanted human array has been a matter of some concern, in part because of some radiological evidence for post-surgical instability of earlier version of the surface ABI. After the array of microelectrodes has been implanted into the patient's brainstem, the proximal end of its cable probably will be subject to considerable manipulation as the cable is routed through the opening in the dura and the dura is closed. Also, the cable may be subjected to additional manipulation as the receiver/stimulator is implanted into its recess in the mastoid bone.

The array system includes two features that are designed to enhance its stability prior to the array and cable being stabilized by the growth of connective tissue. The array itself contains two long (3 mm) iridium stabilizing pins which help to anchor it in the tissue. Secondly, there is a pad of PTFE felt (more recently from PET mesh), 4 x 4 mm on a side and located 6 mm from the array, which is intended to adhere to the surface of the brain. We originally selected the PTFE felt because the surgeons at the House Ear Clinic currently use a tuft of the material to hold the surface ABI in the lateral recess. However, medical-legal issues have caused us to evaluate PET mesh as a substitute.

The flexibility of the cable itself must be carefully considered. If too stiff, the stabliizing pad may lift off of the brain and thus will not be able to stabilize the array when the

cable is manipulated. If the cable is too flexible, the array matrix will flop about while it is being loaded into the inserter tool and the microelectrodes may be damaged.

The stability of the implanted array was evaluated in the cerebral cortex of 3 cats and 4 rabbits. The cortex provides a large surface area upon which the stability of the array and cable can be investigated, without interference from surrounding structures. The arrays were manufactured at HMRI but were fitted with cables manufactured by Cochlear Ltd. This cable has been used with their cochlear implants and with the current version of the ABI, and has proven to be reliable.

After the array was loaded into the barrel of the inserter tool, the underside of the stabilizing pad was wetted with blood. The array was then inserted into the brain and the pad tamped lightly with the end of the tool's barrel, to ensure that its underside was firmly in contact with the brain. Approximately 1 minute was allowed for the blood on the underside of the pad to begin to clot. The stability of the array was then tested by elevating the proximal 10 cm of the cable distal to the pad to a vertical position and by twisting the cable through +/- 90^{O}, so as to apply torque to the stabilizing pad . Our criteria is that the array must not begin to dislodge from the brain, and the matrix must not rock laterally by more than 0.5 mm (20% of its diameter), as determined by a frame-by-frame analysis of the intraoperative video. (We have observed that the array rocks back and forth by approximately 0.5 mm during the brain's normal vascular pulsations). The cable manufactured by Cochlear Ltd satisfied these criteria, for both the PTFE and the PET stabilizing pads.

PUBLICATIONS

The follow publications were supported by this contract, and were published during the contract period

McCreery, D.B., Shannon,R.V., Moore, J.K. and Chategee, M. “Accessing the tonotopic organization of the ventral cochlear nucleus by intranuclear microstimulation.” IEEE Trans. Rehab. Eng., 23(6),391-399,1998.

McCreery, D.B., Yuen, T.G.H., Agnew, W.F. and Bullara, L.A. “Chronic microstimulation in the feline ventral cochlear nucleus: physiologic and histologic effects” . Hearing Research, 149:223-238, 2000